IEEE Access, Volume 8, 2020. pp. 62815-62829
DOI:10.1109/ACCESS.2020.2984488

4D Trajectory Optimization of Commercial Flight for Green Civil Aviation

YONG TIAN[1], XIUQI HE[1,2], YAN XU[3] , LILI WAN[1], AND BOJIA YE[1]

[1]College of Civil Aviation, Nanjing University of Aeronautics and Astronautics, Nanjing 210016, China
[2]Mianyang Branch, Civil Aviation Flight University of China, Mianyang 621051, China
[3]School of Aerospace, Transport and Manufacturing, Cranfield University, Cranfield MK43 0AL, United Kingdom

Corresponding author: Yong Tian (e-mail: tianyong@ nuaa.edu.cn).

This work was supported in part by the National Natural Science Foundation of China under Grant 61671237 and the Natural Science Foundation of Jiangsu Province of China under Grant BK20160798.

ABSTRACT For the current development of green civil aviation, this study aims to optimize the green four-dimensional (4D) trajectory of commercial flight by taking into account conventional cost and environmental cost. Some fundamental models, efficient processing methodologies, and conventional objectives are proposed to construct the framework of trajectory optimization. Based on the environmental cost including greenhouse gas cost and harmful gas cost, green objective functions are presented. The A* algorithm and the trapezoidal collocation method are employed to optimize the lateral path and vertical profile for 4D optimization trajectory generation. A case study for the A320 from Barcelona Airport to Frankfurt Airport yields the results that the optimal costs can be obtained under different objectives and the total cost can be more optimized by adjusting the weights of environmental cost and conventional cost. The study builds an aided tool for 4D trajectory optimization and demonstrates that environmental factors and conventional factors should be taken into comprehensive consideration when constructing the flight trajectory in the future, as well as it can underpin the green and sustainable development of the air transport industry.

INDEX TERMS Air transportation, four-dimensional (4D) trajectory optimization, green civil aviation, environmental cost, visual simulation.

I. INTRODUCTION

With the development of the global air transport industry, the ecological environment issues such as gas emission and greenhouse effect are gradually exposed [1]. The concept of "green civil aviation" has become a new state of the aviation industry to protect the ecological environment and human life and enhanced the ability of sustainable development for modern aviation. Trajectory optimization of commercial flight is a long-term research focus in the civil aviation field [2], [3]. Under the background of vigorously promoting the development of green civil aviation, the environmental protection is integrated into the goal of trajectory optimization [4], and it is practical and far-reaching to build a green 4D optimized trajectory of commercial flight.

For the commercial flight, the most important aviation pollution includes greenhouse gas emissions and noxious gas emissions. How to assess and reduce aviation pollution has been the focus of aviation scholars for a long time. Chapman proposed three methods to alleviate aircraft environmental pollution, that one is to increase the aviation fuel tax imposed by the aviation international agreement, the other is to change the transportation mode, and the third is to upgrade the aircraft design or switch to clean fuel [5]. Yang studied the emission control of international aviation from the perspective of legislation and proposed that international aviation emission should be governed by multi-subject [6].

The management and control of aviation pollution gradually changed from policy and theory to aircraft manufacturing technology improvement and aircraft operation optimization [7]. Timmis et al. developed carbon-fibre-reinforced polymers (CFRP) by the aviation industry to reduce aircraft fuel burn and emissions of greenhouse gases [8]. Moolchandani et al. introduced a developing high-speed environmental assessment tool to evaluate the environmental impact of emissions and noise [9].

Compared with aircraft manufacturing technology improvement, aircraft operation optimization is more efficient. Wei and Wang took into account the influence of atmospheric environment and flight parameters, correcting the emission indices of CO_2, NO_x, CO, and HC generated during flight and assessing the emissions of pollutants at

each stage [10]. Phleps and Hornung proposed a method to calculate the emission cost of noxious gas [11]. Soler et al. proposed a method for calculating the cost of the contrail [12]. Chen et al. developed a strategy to reduce the contrail based on environment and operational cost, linking CO_2 emission and contrail formation to environmental cost through changes of absolute global temperature potential (AGTP) [13], [14].

In the research of trajectory optimization of commercial flight, an aircraft point-mass model was proposed between the six degrees of freedom model and the basic kinematics model, which is considered to be a sufficiently accurate dynamic method for aircraft trajectory planning research [15]. Based on the basic model, Chamlou proposed a new 3-dimensional trajectory collision detection algorithm for judging aircraft position and velocity through ADS-B data and TCAS system [16]. Mou and Wang used the AP model and the GAP model to establish the matrix corresponding to the aircraft and the flight level, so as to obtain the optimal efficiency value of the flight level change scheme through the Hungarian algorithm [17]. Based on the model of historical flight data, Lu fitted the flight altitude profile of the aircraft and used the recursive simulation method to solve the 4D trajectory [18]. Trajectory optimization is inseparable from the application of some new methods and tools. For optimization methods, they include neural network [19], [20], k-means clustering [21], deep learning [22], adaptive fusion and category-level dictionary learning model [23], etc. In terms of optimization tools, GUI (Graphical User Interface) and human-robot interface [24] are increasingly used in the field of trajectory optimization.

At the same time as the basic trajectory research, some scholars have taken environmental factors into consideration. Williams et al. controlled the different flight levels of aircraft through simulation experiments to research the effects of contrail formation and gas emission at different flight levels [25]. Campbell et al. proposed to mitigate the contrail formation by optimizing the aircraft trajectory, and used Mixed Integer Linear Programming (MILP) to solve the model [26]. Sridhar et al. introduced a strategy to reduce the formation of contrails in American airspace [27]. In recent years, some scholars have proposed some new and practical environmental assessment methods for civil aviation. Antonio J. Torija et al. raised a method named Environmental Impact Aviation metric (EIAm) [28]. A. Rodríguez-Díaz et al. established a bi-objective model under Constrained Position Shifting (CPS) restrictions, which minimized noise impact, fuel consumption, and delays [29].

On the basis of considering the environmental protection of the trajectory, the impact analysis on performance model, meteorology model, and high-altitude wind factors was added. Amin and Alam integrated the airspace model, the meteorology model, the continuous contrail model, and the st, which provides reference and guidance for green 4D trajectory optimization of commercial flight from now on.

air route model, and optimized three routes using the gradient descent method [30]. Alizadeh et al. aimed to study an optimal cost index for wind and optimize the arrival trajectory through optimal speed [31]. With the collocation method proposed [32], Codina optimized flight vertical trajectory using Nonlinear Programming (NLP) based on performance models and weather models [33]. Hartjes et al. developed a tool that optimizes the trajectories of multiple airliners that seek to join in formation to minimize overall fuel consumption or direct operating cost [34]. Tian et al. set up an optimal control model to minimize green direct operating cost (GDOC) and established a discrete time dynamic system for optimizing the cruise altitude and speed profiles [35].

At present, scholars' research on the trajectory of commercial flight mainly focuses on the single optimization objective of minimum fuel consumption or minimum emission or conflict resolution, and most of them only study from one dimension such as the lateral path or vertical profile. In the existing studies, more optimization results were analyzed before and after the addition of environmental factors, and fewer horizontal comparisons among other factors and environmental factors were made on trajectory optimization.

In this paper, an efficient and multifunctional tool for green 4D trajectory optimization is built based on the traditional trajectory optimization framework, and horizontal comparisons and a sensitivity study on green objectives and conventional objectives are conducted. Firstly, we develop the trajectory optimization framework and propose the optimization models of conventional objectives for the 4D trajectory. Secondly, through the emission models of greenhouse gases and harmful gases, the concept of environmental cost is proposed, and the green trajectory optimization model for the minimum environmental cost is established. On the account of the green objectives and conventional objectives, a case study for the A320 from Barcelona Airport to Frankfurt Airport is conducted for result analysis and sensitivity study.

The contribution of this research can be divided into three aspects. At first, to improve the practicality of trajectory optimization, a more detailed calculation of the cost in lateral path optimization is made, where accurate wind effects and route charges are computed. Secondly, the objective functions in lateral path optimization and vertical profile optimization are aligned as much as possible by means of relationship between distance and time and establishment of cost functions, in order to build a unified framework for green trajectory optimization in this study. On top of the above two improvements to the trajectory optimization itself, the main contribution is that the concept of environmental cost is proposed based on a set of comprehensive emission metrics to realize as a complementary to the conventional co-

The rest of the paper is organized as follows: Section II elaborates the trajectory optimization framework pertaining

to aircraft dynamics, aircraft performance, air route structures, meteorology, and conventional cost. In Section III how to optimize the green trajectory is introduced. A case study is made and the optimization results are analyzed in Section IV. Finally, Section V presents some conclusions from the study.

II. TRAJECTORY OPTIMIZATION FRAMEWORK

Aircraft dynamics, aircraft performance, air route structure, and meteorology are all indispensable factors for 4D trajectory optimization. In this section, the trajectory optimization framework is established based on the fundamental models in order to build a basic computer-aided tool for 4D trajectory optimization to lay a foundation for generating green optimal trajectories.

A. AIRCRAFT DYNAMICS

The total-energy model equates the rate of work done by forces acting on the aircraft to the rate of increase in potential and kinetic energy, that is:

$$mg\frac{dh}{dt}+mv\frac{dv}{dt}=\left(Thr-D\right)v \tag{1}$$

where m is the mass of the aircraft (kg), g is the local gravity acceleration, v is the true airspeed (TAS) in m/s, Thr is the total thrust and D is the aerodynamic drag; d/dt is the time derivative.Based on the point-mass model proposed by Hull et al., the aircraft motion is reduced to three degrees of freedom (the three translations), assuming that all forces are applied to the center of gravity of the aircraft, where the derivative equations of the three translations can be integrated along the time. Aircraft forces are shown in Figure 1.

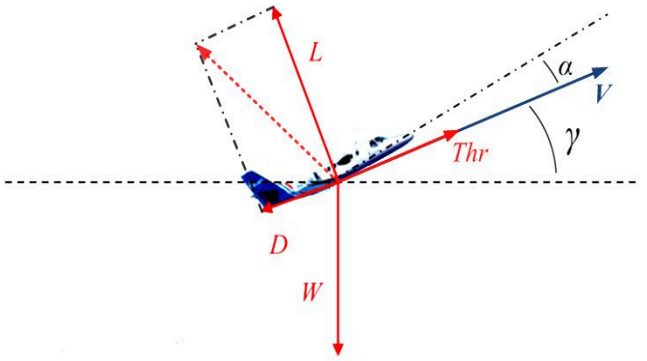

FIGURE 1. **Aircraft force.**

The aerodynamic lift L and drag D are commonly modeled as:

$$L=\frac{1}{2}\rho v^2\cdot C_L\cdot S \tag{2}$$

$$D=\frac{1}{2}\rho v^2\cdot C_D\cdot S \tag{3}$$

where ρ is the density of the air, S is the wing surface area, C_L is the lift coefficient and C_D is the drag coefficient.

The aircraft dynamics models are described in the air reference frame neglecting wind components:

$$\begin{cases}\dfrac{dv}{dt}=\dot{v}=\dfrac{Thr-D}{m}-g\sin\gamma\\ \dfrac{ds}{dt}=\dot{s}=\dfrac{v}{1000}\cos\gamma\\ \dfrac{dh}{dt}=\dot{h}=v\sin\gamma\\ \dfrac{dm}{dt}=\dot{m}=-FF\end{cases} \tag{4}$$

where the state vector $\boldsymbol{x}=[v,\ s,\ h,\ m]$ is formed respectively, by the TAS, the along path distance (km), the flight altitude (m), and the mass of the aircraft (kg); the control vector is $\boldsymbol{u}=[Thr,\ \gamma]$, where γ is the aerodynamic flight path angle; FF is the fuel flow (kg/s).

B. AIRCRAFT PERFORMANCE

Aircraft performance is the parameters that describe the motion law for the aircraft's center of mass, including the speed, altitude, range, duration, take-off, landing, maneuver flight, and so on [36]. The models and parameters of aircraft performance in this paper are all from the Base of Aircraft Data (BADA) published by EUROCONTROL [37]. During the aircraft flight, lift and drag are the two forces that have the greatest impact on aircraft trajectory optimization. Under nominal conditions, the drag coefficient C_D is specified as a function of the lift coefficient C_L as follows:

$$C_D=C_{D_0,CR}+C_{D_2,CR}\cdot\left(C_L\right)^2 \tag{5}$$

where $C_{D_0,CR}$ is the parasitic drag coefficient and $C_{D_2,CR}$ is the induced drag coefficient. The values of two drag coefficients can be obtained in the OPF files of BADA.

The speed of the aircraft is an important parameter for aircraft performance as well. The speed of the aircraft are divided into indicated airspeed (IAS) and true speed (TAS). The calibrated airspeed (CAS) can be got after correcting the installation error and the instrument indication error of IAS and ground speed (GS) is obtained after the correction of the wind speed for TAS. According to BADA, The CAS v_{CAS} and GS v_G for the aircraft are calculated using the following formula:

$$v_{CAS}=\sqrt{\frac{2P_0}{\mu\rho_0}\left[\left(\delta\left(\left(\frac{\mu v^2}{2RT}+1\right)^{\frac{1}{\mu}}-1\right)+1\right)^{\mu}-1\right]} \tag{6}$$

$$v_G = v + v_{wind} \tag{7}$$

$$\mu = \frac{\gamma_a - 1}{\gamma_a} \tag{8}$$

$$\delta = \frac{P}{P_0} \tag{9}$$

where $P_0 = 101,325$ (Pa) is the standard pressure of air, $\rho_0 = 1.225$ (kg/m^3) is the density values at sea level, $R = 287.05287$ (m^2/(K·s^2)) is the perfect gases constant for air, $\gamma_a = 1.4$ is the specific heat ratio of the air; T is the temperature of air and P is the pressure of air; v_{wind} is the wind speed (the downwind is positive). In the actual operation of the flight, the Mach number is also used to reflect the speed of the aircraft. The calculation method of Mach number M in this paper:

$$M = \frac{v}{C} \tag{10}$$

where C is the speed of sound, $C = (\gamma_a RT)^{1/2}$.

Fuel consumption is an important optimization index for aircraft trajectory optimization. For the aircraft of the jet engines, the nominal fuel flow FF_{nom} can be calculated as:

$$FF_{nom} = \eta \times \frac{Thr}{1000} \times \frac{1}{60} \tag{11}$$

$$\eta = C_{f1} \times \left(1 + \frac{v}{C_{f2}}\right) \tag{12}$$

where η is the thrust specific fuel consumption, C_{f1} is the first thrust specific fuel consumption coefficient and C_{f2} is the second thrust specific fuel consumption coefficient. This expression is used in all flight phases except during idle descent and cruise. The idle descent is neglected in this paper, so the formula of the fuel flow during the cruise is:

$$FF_{cr} = \eta \times \frac{Thr}{1000} \times C_{fcr} \times \frac{1}{60} \tag{13}$$

where C_{fcr} is the cruise fuel flow correction coefficient.

C. AIR ROUTE STRUCTURES

1) WAYPOINTS

To achieve 4D trajectory optimization of commercial flight, the data of waypoint in the airspace is essential. The data of waypoint mainly includes the longitude of waypoints, the latitude of waypoints and the connection relationship among waypoints, so as to obtain the basic structure. In this paper, the north latitude and the east longitude is positive. Since this paper only focuses on the 4D trajectory optimization between the two city pairs, it is unnecessary to consider the operation of the aircraft in the terminal area, so the departure airport and arrival airport are approximately regarded as a waypoint. The data of waypoint is within the European airspace in the paper, and the network of the air routes for Europe is shown in Figure 2.

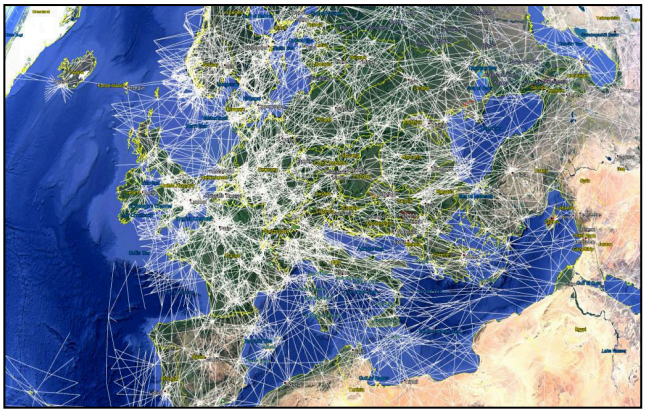

FIGURE 2. The network of the air routes for Europe.

2) FLIGHT SECTORS

The data of flight sectors in this paper is mainly composed of the latitude and longitude coordinates of the boundary of several airblocks, the airblocks contained in each sector and the en route charges of sectors.

This paper introduces the concept of HOTSPOT, which refers to a busy sector where the flow and capacity are unbalanced in a certain period [38]. The controller load and the probability of flight collision in HOTSPOT are both higher, so flying around HOTSPOT is an important optimization target. Line Intersecting Method (LIM) is proposed to determine whether an intersection occurs between the segment of two waypoints and the boundary of each airblock in one sector in order to realize the fly-around for HOTSPOT. In order to improve the efficiency of judgment, the LIM is divided into two steps of rectangle judgment and cross-product judgment, as shown in Table I. It is assumed line segment AB is one of the segments between two waypoints and line segment CD is one segment of one airblock's boundary. According to the rectangle judgment, when the rectangle formed with AB as the diagonal and the rectangle formed with CD as the diagonal do not overlap, the two line segments are inevitably unable to intersect, so the LIM can finish in advance to improve the efficiency of judgment. If rectangle judgment passes, the cross-product judgment will start, which is also called the straddle judgment. Only when the two points of AB straddle both sides of CD, the line segment AB intersects the line segment CD.

TABLE I
DIAGRAM OF RECTANGLE JUDGMENT AND CROSS-PRODUCT JUDGMENT OF LIM

Rectangle Judgment / Cross-product Judgment	Pass	No Pass
No Pass	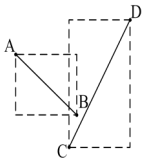	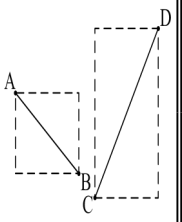
Pass	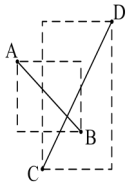	

Besides the fly-around of HOTSPOT, the en route charge is another data that needs to be processed. Generally, the segment between two waypoints crosses one or two sectors. Thus, the en route charge unit rate of the whole segment is obtained by calculating the average value of the unit rate of sectors where the front and rear waypoints are located. Since the sectors are some irregular polygons composed of airblocks, Ray Casting Method (RCM) is adopted in this paper to determine the sectors where the waypoints are located. RCM leads a ray from the target point. If the number of intersections between the ray and the polygon boundary is odd, the point is inside the polygon; otherwise, the number of intersections is even or zero, the point is outside the polygon, as shown in Figure 3. In the same way, the airblocks of sectors includes the starting and ending waypoint of a segment are determined to obtain en route charges of one segment.

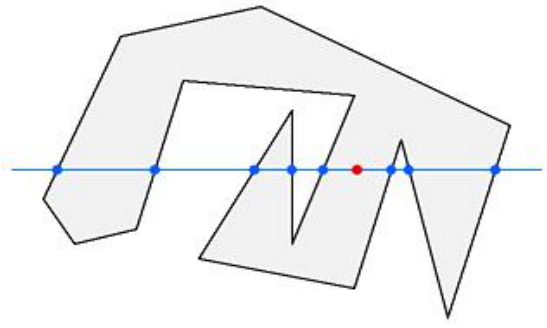

FIGURE 3. **Diagram of RCM.**

If the waypoint is on the boundary of the sector, the sector may not be determined accurately where the waypoint is located by RCM. Therefore, Adduction Method (AM) is put forward to solve the special situation of the waypoint on the boundary. The expression of the AM is:

$$x'_k = \begin{cases} x_k + \left(x_{rear} - x_{front}\right)/\varsigma, \\ \quad k \text{ is } front \text{ and the front} \\ \quad \text{waypoint is on the boundary} \\ x_k - \left(x_{rear} - x_{front}\right)/\varsigma, \\ \quad k \text{ is } rear \text{ and the rear} \\ \quad \text{waypoint is on the boundary} \end{cases} \tag{14}$$

$$y'_k = \begin{cases} y_k + \left(y_{rear} - y_{front}\right)/\varsigma, \\ \quad k \text{ is } front \text{ and the front} \\ \quad \text{waypoint is on the boundary} \\ y_k - \left(y_{rear} - y_{front}\right)/\varsigma, \\ \quad k \text{ is } rear \text{ and the rear} \\ \quad \text{waypoint is on the boundary} \end{cases} \tag{15}$$

where k is the marks of the front and rear waypoints of one segment (we defined the start waypoint is the front waypoint and the end waypoint is the rear waypoint when the aircraft flies through one segment), x_k is the original x coordinate of the waypoint, y_k is the original y coordinate of the waypoint, x'_k is the new x coordinate of the waypoint after adduction, y'_k is the new y coordinate of the waypoint after adduction, x_{front} and y_{front} are the x coordinate and the y coordinate of the front waypoint, x_{rear} and y_{rear} are the x coordinate and the y coordinate of the rear waypoint, and ς is adduction coefficient. The larger the adduction coefficient is, the less the adduction is and the higher the adduction accuracy is. Because of the large range of sectors, high adduction accuracy is not required in this paper, so it is assumed that $\varsigma = 100$.

D. METEOROLOGY

Meteorology is the interdisciplinary scientific study of the atmosphere. For aircraft trajectory optimization research, the main atmospheric properties are temperature, pressure, the density of the air and relative humidity. In the international standard atmosphere (ISA) model of BADA, ISA temperature gradient with the altitude below the tropopause is $\beta = -0.0065$ (K/m) and the ISA temperature of the standard sea level is $T_0 = 288.15$ (K). The altitude of the tropopause is $h_{trop} = 11,000$ (m) in the ISA model and the temperature is considered constant above the tropopause:

$$T = \begin{cases} T_0 + \beta \cdot h, & h \le h_{trop} \\ T_{trop}, & h > h_{trop} \end{cases} \tag{16}$$

where T_{trop} is the temperature of the tropopause (K). The pressure is calculated using the following formula:

$$P = \begin{cases} P_0 \left(\dfrac{T}{T_0} \right)^{-\frac{g}{\beta \cdot R}}, & h \le h_{trop} \\ P_0 \left(\dfrac{T_{trop}}{T_0} \right)^{-\frac{g}{\beta \cdot R}} \cdot \exp\left[-\dfrac{g}{RT_{trop}} \left(h - h_{trop} \right) \right], & h > h_{trop} \end{cases} \tag{17}$$

Finally, the air density is calculated from the pressure and the temperature at altitude using the perfect gas law:

$$\rho = P / RT \tag{18}$$

The data of weather in this paper is mainly derived from the GRIB2 files published by Global Forecast System (GFS) of National Oceanic and Atmospheric Administration (NOAA), and the GFS data is further divided into GFS Analysis data and GFS Forecasts data. As shown in Figure 4, the weather data of the 1° × 1° latitude and longitude grid is selected in the GFS Analysis data.

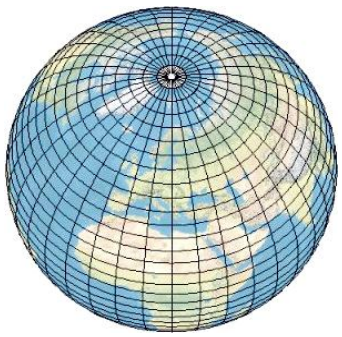

FIGURE 4. Diagram of the grid of latitude and longitude.

Based on the LIM, this paper introduces an intersection method for line segment and rectangle to determine which grids of latitude and longitude the segment crosses, as shown in Figure 5. The intersection method for line segment and rectangle is divided into two steps. Firstly, the grids of the waypoints at both ends of the segment are determined, and then the diagonal of the grid intersecting the segment is judged according to the LIM, so as to judge which grids of latitude and longitude the whole segment crosses.

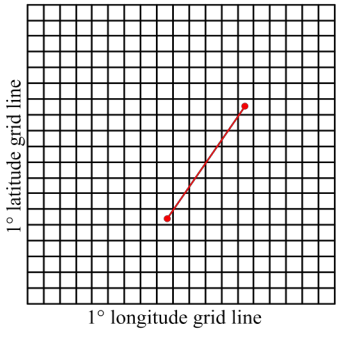

FIGURE 5. Segment crosses the 1°×1° grids of latitude and longitude.

The certain same weather data value (such as temperature, pressure, relative humidity, wind direction, and wind speed, etc.) of the longitude and latitude grids crossed by the segment between two waypoints is summed and averaged, in order to obtain the weather data value of the whole segment, and the function is expressed as:

$$Wea_{ab} = \frac{\sum_{n=1}^{N} Wea_n}{N} \tag{19}$$

where Wea_{ab} is the certain weather data value of one segment with starting waypoint a and ending waypoint b , n is the mark of grids which the segment crosses, N is the total number of grids crossed by the segment.

E. CONVENTIONAL COST FUNCTIONS

In the paper, the concept of conventional cost means the sum of fuel cost, time cost, and en route charges. We proposed the models of conventional objectives including the shortest distance, the shortest flight time, and the minimum conventional cost to perform fundamental optimization of the 4D trajectory.

1) FUEL COST

Fuel cost is an important factor in the trajectory optimization of commercial flight. Considering the impact of high-altitude wind in this paper, the fuel cost is related to flight distance, TAS, wind speed, fuel flow, and fuel cost coefficient:

$$Cost_{fuel} = \frac{1000 \cdot s}{v + v_{wind}} \cdot FF \cdot C_F \tag{20}$$

where $Cost_{fuel}$ is the fuel cost (€) and C_F =0.8 (€/kg) is the fuel cost coefficient.

2) TIME COST

The time cost of the flight includes ownership cost, maintenance cost, and crew cost. Based on the cost index, the time cost can be calculated as:

$$Cost_{time} = CI \cdot C_F \cdot t / 60 \tag{21}$$

where $Cost_{\text{time}}$ is the time cost (€) and t is the time of the flight (s).

3) EN ROUTE CHARGES

During the cruise flight, the aircraft flies over different sectors, and the en route charges of different sector zones are considered, which can influence the trajectory optimization. A model of the en route charges is proposed in the Customer Guide to Charges of July 2019 [39]:

$$Cost_{charge} = d \cdot u_r \cdot \sqrt{\frac{MTOW}{50}} \tag{22}$$

where $Cost_{charge}$ is the en route charges (€), d is the distance factor and is obtained by dividing by one hundred the numb-

er of kilometers flown in the great circle distance of each segment, $MTOW$ is the maximum take-off weight (t), and u_r is the en route charging zone unit rate of Europe. The unit rate is updated every month by EUROCONTROL, and the unit rate of September 2019 is shown in Table II.

TABLE II
EUROCONTROL MEMBER STATES' NATIONAL UNIT RATES IN €

ICAO Code of Sector Zone	The Unit Rate of En Route Charges	ICAO Code of Sector Zone	The Unit Rate of En Route Charges	ICAO Code of Sector Zone	The Unit Rate of En Route Charges
AZ	9.67	EY	42.89	LM	22.51
EB	67.69	GC	49.96	LO	67.88
ED	63.77	LA	50.6	LP	24.82
EE	29.31	LB	31.42	LQ	34.74
EF	50.02	LC	31.98	LR	29.9
EG	56.96	LD	42.55	LS	97.82
EH	56.91	LE	61.33	LT	22.42
EI	28.26	LF	60.95	LU	59.01
EK	57.15	LG	30.59	LW	45.72
EN	42.41	LH	30.02	LY	29.62
EP	40.39	LI	78.1	LZ	49.83
ES	49.6	LJ	59.65	UD	29.96
EV	27.16	LK	40.03	UG	21.06

4) CONVENTIONAL OBJECTIVES

According to the aircraft dynamics, the aircraft performance, air route structure, and meteorology, this section constructs the initial models for the shortest distance and the shortest flight time under HOTSPOT fly-around, which can be described as:

$$\min F_{distance} = \sum \left[\min \left(s_j \right) \right], \ j \notin Close, j \in Seg \tag{23}$$

$$\min F_{time} = \min \sum \left(t \right) \tag{24}$$

where s_j is the distance of segment j, $Close$ is the set of segments which are in HOTSPOTs, Seg is the set of all the segments.

The model for the objective of the minimum conventional cost under HOTSPOT fly-around is:

$$\begin{aligned} \min C_{conventional} = \min \Big[\sum \big(& Cost_{j,fuel} + Cost_{j,time} \\ & + Cost_{j,charge} \big) \Big], \ j \notin Close, j \in Seg \end{aligned} \tag{25}$$

where $Cost_{j,fuel}$, $Cost_{j,time}$, and $Cost_{j,charge}$ are fuel cost, time cost, and en route charges of the segment j.

III. GREEN TRAJECTORY GENERATION

The conventional objectives mentioned in the previous section are not considering the environmental impacts, which is not enough. Environmental issues such as emissions, noise, and the greenhouse effect have become important factors limiting the development of the global civil aviation industry, so the research of green civil aviation has become a new focus for many aviation scholars. This paper focuses on the greenhouse gases of CO_2 and contrail and the harmful gases of HC, CO, and NO_x, and the concept of the environmental cost is presented to optimize the trajectory for green civil aviation.

A. EMISSION MODELS

First of all, the emission models of gases based on the emission indices are put forward here.

For the greenhouse gases, CO_2 emissions E_{CO_2} of commercial flight are related to CO_2 emission index EI_{CO_2} and fuel consumption FB in kilogram [40]:

$$E_{CO_2} = EI_{CO_2} \cdot FB \tag{26}$$

where $EI_{CO_2} = 3.155$ (kg/kg). Contrails form in the regions of airspace that have ambient relative humidity with respect to water RH_W greater than a critical value $R_{critical}$. Contrails can persist when the environmental relative humidity with respect to ice RH_i is greater than 100%. According to the relevant formula [41], it is judged whether the atmospheric condition meets the two conditions of the end of condensation: (a) $R_{citical} \le RH_W < 100\%$; (b) $RH_i \ge 100\%$.

For the harmful gases, the emission models are:

$$E_{HC} = EI_{HC} \cdot FB \tag{27}$$

$$E_{CO} = EI_{CO} \cdot FB \tag{28}$$

$$E_{NO_x} = EI_{NO_x} \cdot FB \tag{29}$$

where E_{HC}, E_{CO}, and E_{NO_x} are emissions of HC, CO, and NO_x; EI_{HC}, EI_{CO}, and EI_{NO_x} are emission indices of HC, CO, and NO_x (g/kg). Different engines for different aircraft correspond to different emission indices of the harmful gases, which can be obtained through ICAO Aircraft Engine Emissions Databank (EDB) from European Union Aviation Safety Agency (EASA). The emission indices of the harmful gases for some aircraft are listed in Table III. All the indices in Table III are measured according to the procedures in ICAO Annex 16, Volume II [42] and certified by the States of Design of the engines according to their national regulations. Chen et al. [41] and Tian et al. [43] used the same data source to realize the reduction of the emissions in the airspace.

TABLE III
THE EMISSION INDICES OF THE HARMFUL GASES FOR SOME AIRCRAFT

Aircraft	EI_{HC}	EI_{CO}	EI_{NO_x}	Aircraft	EI_{HC}	EI_{CO}	EI_{NO_x}
A306	0.02	0.54	23.7	B733	0.05	0.95	15.5
A310	0.11	0.56	20.71	B734	0.05	0.95	15.5
A318	0.1	0.8	17.9	B735	0.05	0.95	15.5
A319	0.11	0.55	30.82	B736	0.02	0.17	17.89
A320	0.2	0.9	21.1	B737	0.02	0.17	17.89
A321	0.1	0.5	27.2	B738	0.02	0.17	17.89
A332	0.01	0.49	26.82	B739	0.02	0.17	17.89
A333	0.07	0.34	28.02	B742	0.14	0.63	30
A343	0.008	0.85	29.05	B743	0.05	0.04	19.68
A345	0.01	0.44	30.98	B744	0.07	0.5	25.98
A346	0.01	0.38	33.25	B752	0.02	0.34	23.96
A388	0	0.54	11.39	B753	0	0.6	36.82
B77L	0.03	0.07	33.85	B762	0.14	0.63	30
B77W	0.03	0.07	35.98	B763	0.06	0.49	25.03
B703	0.1	0	28.5	B764	0.14	0.63	29.5
B712	0.03	0.66	13.93	B772	0.03	0.31	40.63
B722	0	0.46	13.73	B773	0.03	0.31	40.63
B732	0.18	1.11	14.5	-	-	-	-

B. ENVIRONMENTAL COST FUNCTIONS

Compared with the current various environmental assessment methods, the concept of environmental cost is used to combine environmental protection and economic efficiency in this paper. The environmental cost includes the cost of greenhouse gases $Cost_{greenhouse}$ and the cost of harmful gases $Cost_{harmful}$, and the cost of greenhouse gases consists of the cost of CO_2 emissions and the cost of contrail formation, while the cost of harmful gases is the amount of the emission costs of HC, CO, and NO_x.

1) GREENHOUSE GAS COST

The time cost of the flight includes ownership cost, maintenance cost, and crew cost.This paper attempts to relate AGTP due to CO_2 emissions and aircraft contrails to the environmental cost in Euro. Using the social cost of carbon dioxide as an estimate of the environmental cost of CO_2 due to warming:

$$Cost_{CO_2} = SCC \cdot \frac{E_{CO_2}}{1000} \tag{30}$$

where $Cost_{CO_2}$ is the cost of CO_2 emissions (€) and the social cost of carbon SCC is about 22.83 (€/t) at present proposed by National Bureau of Economic Research (NBER) [44]. In order to quantify the environmental cost of contrails, the environmental cost of temperature changes, specifically one Kelvin of AGTP, was defined using the SCC and the AGTP coefficient of CO_2 for time horizon H years:

$$ECK = \frac{SCC}{1000 \cdot \alpha(H)} \tag{31}$$

where ECK is the equivalent environmental cost of temperature change (€/K) and $\alpha(H)$ is the AGTP coefficient of CO_2 for the time horizon of H years. Using the ECK to relate the environmental cost from contrails to CO_2 assuming that the same temperature change of CO_2 and temperature change of contrail have the same environmental cost for the time horizon of H years, $Cost_{Con}$ can be formulated as:

$$Cost_{Con}^{H} = ECK \cdot \Delta T_{Con}(H) = \frac{SCC}{1000} \cdot \frac{\beta(H)}{\alpha(H)} \cdot L_{Con} \tag{32}$$

where L_{Con} is the contrail length (km), and $\beta(H)$ is the AGTP coefficient of contrails for the time horizon of H years. A list of $\alpha(H)$ and $\beta(H)$ is shown in Table IV [14].

TABLE IV
AGTP COEFFICIENTS FOR CO_2 AND CONTRAILS FOR THREE DIFFERENT TIME HORIZONS

Time Horizon	$H = 25$ years	$H = 50$ years	$H = 100$ years
$\alpha(H)$, K/kg	6.71×10^{-16}	5.78×10^{-16}	5.07×10^{-16}
$\beta(H)$, K/km	1.48×10^{-13}	6.98×10^{-15}	5.10×10^{-15}

According to the functions above, the model of the greenhouse gas cost can be expressed as:

$$Cost_{greenhouse} = Cost_{CO_2} + Cost_{Con}^{H} \tag{33}$$

2) HARMFUL GAS COST

Compared with the costs of greenhouse gases, the costs of harmful gases HC, CO, and NO_x are more uniform. The calculation formula for the emission costs of harmful gases is proposed by Phleps and Hornung [11]:

$$Cost_{HC} = (E_{HC} / 1000000) \cdot C_U \cdot f_{emission} \tag{34}$$

$$Cost_{CO} = (E_{CO} / 1000000) \cdot C_U \cdot f_{emission} \tag{35}$$

$$Cost_{NO_x} = (E_{NO_x} / 1000000) \cdot C_U \cdot f_{emission} \tag{36}$$

where $Cost_{HC}$, $Cost_{CO}$, and $Cost_{NO_x}$ are emission costs of HC, CO, and NO_x (€), $C_U = 4$ (€/t) is the harmful gas emission cost coefficient and $f_{emission} = 15.9\%$ is the percentage of the flights affected by emission charges. Therefore, the model of the harmful gas cost is:

$$Cost_{harmful} = Cost_{HC} + Cost_{CO} + Cost_{NO_x} \tag{37}$$

3) GREEN OBJECTIVES

For green trajectory generation, based on the models of environmental costs, the objective function for the minimum environmental cost under HOTSPOT fly-around can be expressed as:

$$\min C_{environmental} = \min\left[\sum (Cost_{j,greenhouse} + Cost_{j,harmful})\right],\ j \notin Close,\ j \in Seg \tag{38}$$

where $Cost_{j,greenhouse}$ and $Cost_{j,harmful}$ are greenhouse gas cost and harmful gas cost of the segment j .

Based on the models of conventional costs and environmental costs, the fourth objective function for the minimum total cost under HOTSPOT fly-around is proposed in this paper:

$$\min C_{total} = \min\left(C_{conventional} + C_{environmental}\right),\ j \notin Close,\ j \in Seg \tag{39}$$

C. LATERAL PATH OPTIMIZATION

In order to construct the green 4D trajectory, the lateral path is optimized at first. For standardizing the lateral path optimization process and facilitating the problem description, the following assumptions are made for the optimization: (1) the aircraft is treated as a particle; (2) take-off and landing airports are treated as two waypoints; (3) in the optimization, the standard cruise Mach number, rated TAS and rated fuel flow of aircraft in the PTF files of BADA are used.

The A* (A-Star) algorithm is used to optimize the lateral path, which is the most effective heuristic direct search method for solving the problems of the shortest paths in stati-

c networks. Compared with the depth-first search, which cannot find the optimal solution, and breadth-first search, which requires higher time complexity and space complexity, the A* algorithm uses the heuristic search to find the optimal solution with maximum probability and reduce redundant time.

The closer the estimated value in the A* algorithm is to the actual value, the faster the final search speed is, and the optimization result is much closer to the optimal solution. The algorithm expression is

$$f(n)=g(n)+h(n) \tag{40}$$

where $f(n)$ is the total cost from the initial state via state n to the target state, which is the total distance of the flight or the total cost of the flight in lateral path optimization; $g(n)$ is the actual cost from the initial state to the state n in the state space, which is the actual distance or cost of each segment; $h(n)$ is the estimated cost for the optimal path from state n to the target state, which is the estimated minimum distance or cost of each waypoint to the destination airport. The A* algorithm for lateral path optimization is shown in **algorithm 1**.

Algorithm 1 The Process of A* Algorithm for Lateral Path Optimization

Input: code of departure airport, arrival airport, and HOTSPOTs

Output: total cost and the corresponding lateral path

Initialize take the departure airport as the current point and add the current point to the set of connectable points

1: **loop while** the set of connectable points is not empty
2: Select the connection point with the minimum total cost in the set of connectable points and take it as the current point
3: **if** current point = arrival airport **then**
4: Output total cost and lateral path
5: **loop while** all points not in HOTSPOTs that are connectable to the current point
6: Calculate the actual cost and estimated cost between the current point and the connectable point
7: Put the connectable point into the set of connectable points
8: **end of loop**
9: **end of loop**

D. VERTICAL PROFILE OPTIMIZATION

On the basis of lateral path optimization, the vertical profile is further optimized. The following assumptions are made for the vertical profile optimization: (1) the influence of the wind is not taken into account; (2) the clean configuration of aircraft is selected to optimize; (3) an estimation is done for the value of the aircraft initial state, based on historical data from previous simulations.

In this paper, the vertical profile optimization of the aircraft is implemented by trapezoidal collocation method. The original continuous-time problem statement of trajectory is converted into a Mixed-Integer Nonlinear Program (MINLP) through trapezoidal collocation method, and then obtain the optimized vertical profile through solving MINLP. The method diagram is shown in Figure 6. The time horizon is divided into several time intervals called phases, and each phase is divided into several discretization steps t, where $x^{(phase)}\left(t_k^{(phase)}\right)$ represents the aircraft state of the discretization step k in one phase, which should meet the function $x^{(phase)}\left(t_f^{(phase)}\right)=x^{(phase)}\left(t_0^{(phase)}\right)$ (t_0 is the first step and t_f is the last step of each phase).

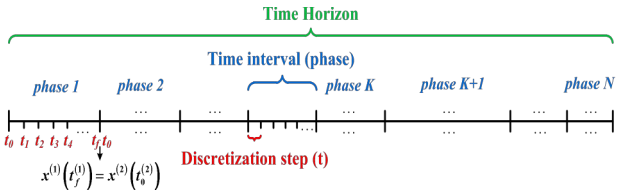

FIGURE 6. **Discretization process for vertical profile optimization.**

In this paper, the vertical profile is divided into 14 phases to discretize the trajectory, so as to get a limited set of decision variables. Then, the conventional operations trajectory model is treated as a set of constraints that can be applied to the path constraints and event or box constraints, as shown in Table V. In Table V, $\dot{v}_{CAS}(t)$ is the derivative of CAS, $h(t_0)$ is the starting height of climb acceleration and the ending height of descent deceleration (m), VMO is the maximum CAS (m/s), MMO is the maximum Mach, $\Delta t_{\min}^{(cruise)}$ is minimum flight time during the phase of cruise (s) and $\Delta s_{\min}^{(cruise)}$ is minimum flight distance during the phase of cruise (km). For this paper, it is considered $\Delta t_{\min}^{(cruise)}=300$ (s) and $\Delta s_{\min}^{(cruise)}=92.6$ (km). According to FAA and EASA regulations, a minimum rate of climb of $ROC_{\min}=2.54$ m/s is enforced to all aircraft in order to ensure that controllers can predict flight profiles to maintain standard separation.

According to trapezoidal collocation method, the function of fuel consumption can be expressed as:

$$\int_{t_0^{(1)}}^{t_f^{(14)}} FF(t)\,dt \approx \sum_{phase=1,t=t_0}^{phase=14,t=t_f} \frac{1}{2}\left(FF_{phase,t}+FF_{phase,t+1}\right)\cdot\Delta t \tag{41}$$

where $FF(t)$ is the fuel flow of discretization step t and Δt is the interval between two steps.

TABLE V
PATH CONSTRAINTS AND EVENT OR BOX CONSTRAINTS FOR 14 PHASES

Phase	Description	Path Constraints	Event or Box Constraints
1	Initial acceleration	$\dot{v}_{CAS}(t) \geq 0$	
2	Constant CAS climb	$v_{CAS}(t) \leq 125$ m/s	
3	Climb acceleration	$\dot{v}_{CAS}(t) \geq 0$	$h(t_0) = 3,048$ m
4	Constant CAS climb	$v_{CAS}(t) \leq VMO$	
5	Constant Mach climb	$M(t) \leq MMO$	
6	Cruise	$M(t) \leq MMO$ $h(t) = (2p_h^{(6)} + 1) \cdot 304.8$ m ; $14 \leq p_h^{(6)} \leq 19$	$t_f \geq t_0 + \Delta t_{\min}^{(cruise)}$ $s(t_f) \geq s(t_0) + \Delta s_{\min}^{(cruise)}$
7	Step climb	$M(t) \leq MMO$	$t_f \leq t_0 + (h^{(8)} - h^{(6)}) / ROC_{\min}$
8	Cruise	$M(t) \leq MMO$ $h(t) = (2p_h^{(8)} + 1) \cdot 304.8$ m ; $14 \leq p_h^{(8)} \leq 19$	$t_f \geq t_0 + \Delta t_{\min}^{(cruise)}(p_h^{(8)} - p_h^{(6)})$ $s(t_f) \geq s(t_0) + \Delta s_{\min}^{(cruise)}(p_h^{(8)} - p_h^{(6)})$
9	Cruise deceleration	$M(t) \leq MMO$ $h(t) = (2p_h^{(9)} + 1) \cdot 304.8$ m ; $14 \leq p_h^{(9)} \leq 19$	
10	Constant Mach descent	$M(t) \leq MMO$	
11	Constant CAS descent	$v_{CAS}(t) \leq VMO$	
12	Descent deceleration	$\dot{v}_{CAS}(t) \leq 0$	
13	Constant CAS descent	$v_{CAS}(t) \leq 125$ m/s	$h(t_0) = 3,048$ m
14	Final deceleration	$\dot{v}_{CAS}(t) \leq 0$	

IV. CASE STUDY

This section employs a case study by using the proposed trajectory optimization framework and methods to compare the results of different objective functions and verify the feasibility of green 4D trajectory optimization.

A. SIMULATION SETUP

In terms of aircraft performance, the A320 is selected as the aircraft type for this case study, and the performance parameters of A320 are obtained from BADA shown in Table VI.

TABLE VI
PERFORMANCE PARAMETERS OF A320

Performance parameters	Value
Standard cruise Mach number	0.78
The first thrust specific fuel consumption coefficient C_{f1} (kg/(min·kN))	0.6333
The second thrust specific fuel consumption coefficient C_{f2} (m/s)	429.515
The cruise fuel flow correction coefficient C_{fcr}	0.95423
Wing surface area S (m^2)	122.4
The parasitic drag coefficient $C_{D0,CR}$	0.025149
The induced drag coefficient $C_{D2,CR}$	0.036138
The reference mass m (kg)	64,000

For the air route structure, this case study chooses the airport pair in Europe from LEBL (Barcelona Airport) to EDDF (Frankfurt Airport) as the test site. The preset cruising altitude is 11,900 m. The sectors named LFMMML and LFFFHP is preset as two HOTSPOTs. The data of en route charging zone unit rate for the whole sectors are from September 2019 as shown in Table II.

The weather data of September 1, 2019, at UTC 00 is chosen for this case study. The time horizon of AGTP coefficients for CO_2 and contrails is set to 100 years.

In this section, each phase is divided into 20 discretization steps t for vertical profile optimization.

The program for lateral path optimization is written on JetBrains PyCharm Community Edition 2019.1.3 x64 in the Python language and the solver of GAMS on GAMS Studio win64 25.1.3 is used to optimize the vertical profile. Visual simulation is realized on Google Earth in the KML language.

B. NUMERICAL RESULTS

The trajectory optimization tool constructed in this paper is capable of generating all the types of trajectories, being the two trajectories of conventional objectives as the benchmark of the case study. In order to facilitate the distinction and expression, this paper uniformly names the objective of the shortest flight distance under HOTSPOT fly-around for later-

al path optimization (the objective of the shortest flight time for vertical profile optimization) as Objective 1, the objective of the minimum conventional cost as Objective 2, the objective of the minimum environmental cost as Objective 3, and the minimum total cost as Objective 4.

According to the optimization models of four objectives, the A* algorithm is applied to optimize the lateral paths. The optimized results are shown in Figure 7.

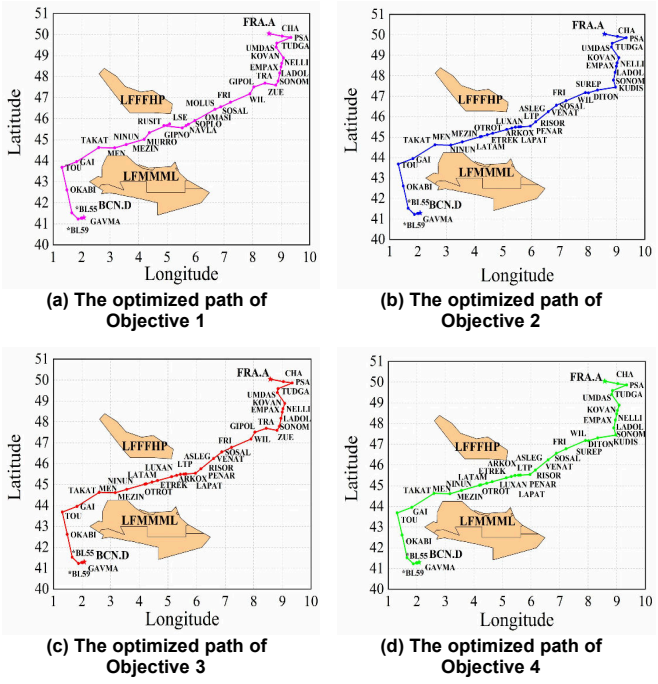

FIGURE 7. **The optimized lateral paths of four objectives.**

Based on the optimization results, the optimized lateral paths of four objectives are visualized on the Google Earth platform as shown in Figure 8.

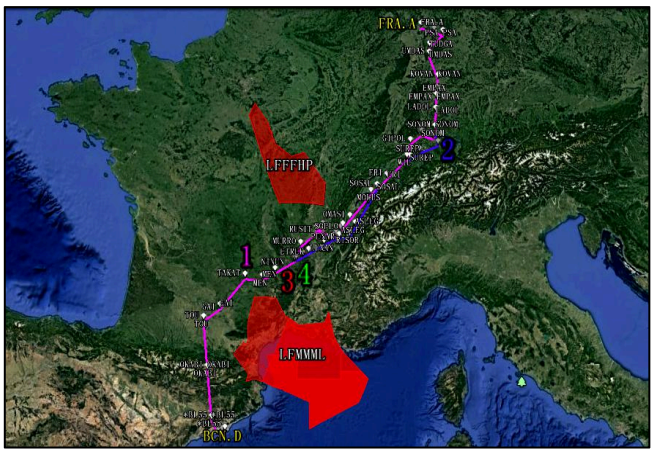

FIGURE 8. **The visual simulation of the optimized lateral paths of four objectives.**

On the basis of the optimization results shown in Table VII, when considering the shortest flight distance under HOTSPOT fly-around, not only conventional cost, environmental cost and total cost are higher, but also because of the deviation between the estimated value and the actual value of A* algorithm, the optimal flight distance cannot be obtained. In this case, the optimal total cost is derived from optimal conventional cost, while if the minimum environmental cost is obtained, the more conventional cost of the lateral path is needed compared with the optimal conventional cost.

TABLE VII
THE RESULTS OF THE LATERAL PATH OPTIMIZATION

	Conventional cost (€)	Environmental cost (€)	Total cost (€)	Flight distance (km)
Objective 1	6,844.39	277.64	7,122.03	1,455.91
Objective 2	6,627.36	268.86	6,896.22	1,409.00
Objective 3	6,628.78	268.76	6,897.54	1,410.02
Objective 4	6,627.36	268.86	6,896.22	1,409.00

The distances of the optimized lateral path are treated as the horizontal reference for vertical profile optimization. Four sets of the height profile diagram, the speed profile diagram and the cumulative time diagram for the vertical profile optimization are shown in Figure 9 to Figure 12.

Figure 9 shows that when based on the Objective 1, the aircraft reaches the TOC (Top of Climb) at 432 km and the TOD (Top of Descent) at 1300 km. The cruise altitude remains at 8839.2 m and the maximum flight speed reaches 237.78 m/s at 226 km. The total flight time from Barcelona airport to Frankfurt airport is 110.05 min.

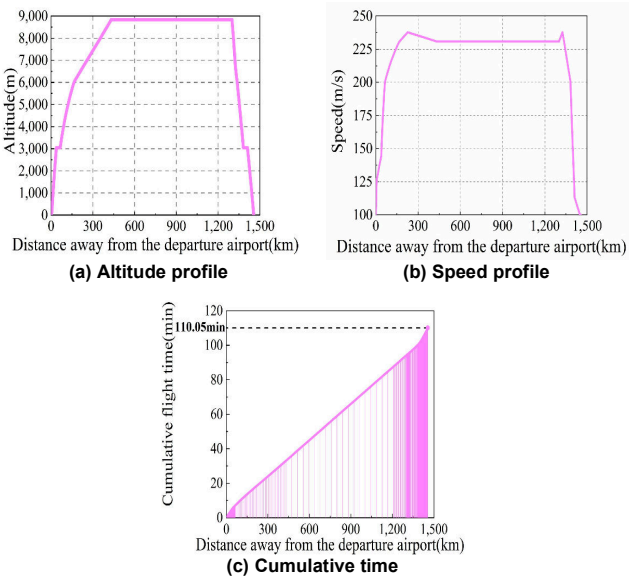

FIGURE 9. **The optimized vertical profile of Objective 1.**

As shown in Figure 10, when based on the Objective 2, the aircraft reaches the TOC at 306 km and the TOD at 1209 km. The cruise altitude remains at 11887.2 m and the maximum flight speed reaches 228.69 m/s at 197 km. The total flight time is 111.2 min.

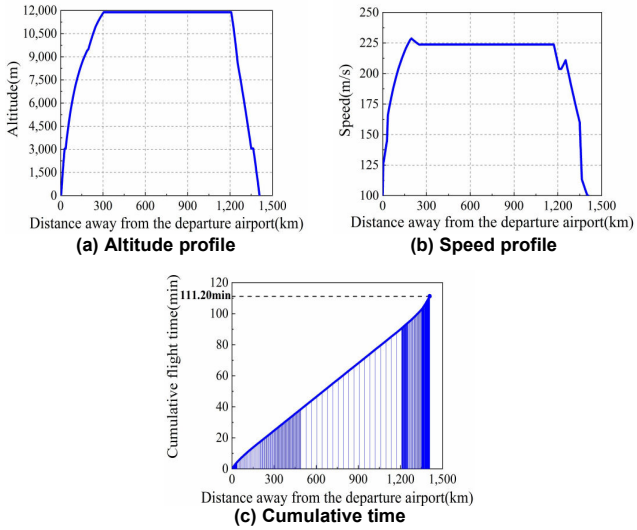

FIGURE 10. **The optimized vertical profile of Objective 2.**

In Figure 11, it is shown that when based on the Objective 3, the aircraft reaches the TOC at 267 km and the TOD at 1178 km. The cruise altitude remains at 11887.2 m. In order to obtain the minimum environmental cost, the flight speed increases to 212.28 m/s and then continues to increase to 223.69 m/s. The total flight time from Barcelona airport to Frankfurt airport is 119.79 min.

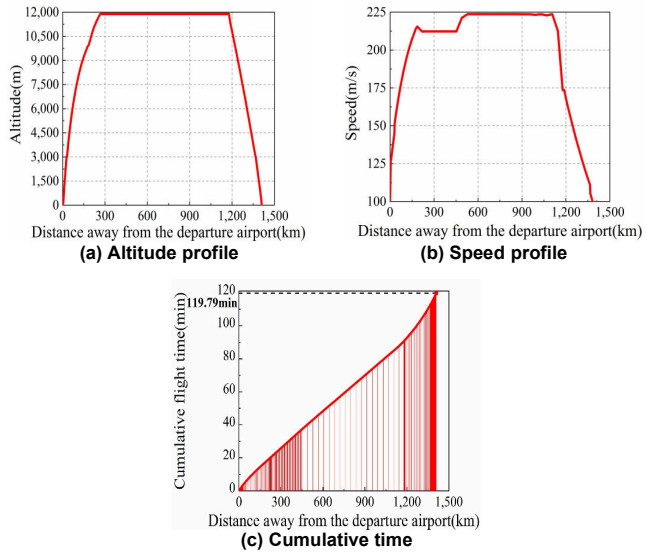

FIGURE 11. **The optimized vertical profile of Objective 3.**

As shown in Figure 12, when based on the Objective 4, the aircraft reaches the TOC at 306 km and the TOD at 1208 km. The cruise altitude remains at 11887.2 m and the maximum flight speed reaches 228.67 m/s at 197 km. The total flight time is 111.22 min.

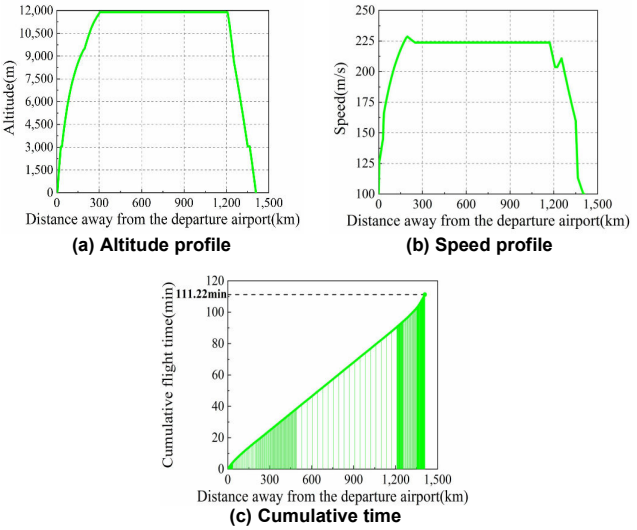

FIGURE 12. **The optimized vertical profile of Objective 4.**

The optimization results are displayed in Table VIII, and it is shown that the shortest flight time can be got when the higher costs are paid. Meanwhile, the results also show that, by comparing the results of Objective 3 with the results of Objective 2 and 4, it is found that for obtaining the optimal environmental cost, the longer flight time and the more conventional cost are needed to spend.

TABLE VIII
THE RESULTS OF THE VERTICAL PROFILE OPTIMIZATION

	Conventional cost (€)	Environmental cost (€)	Total cost (€)	Flight time (min)
Objective 1	7,565.92	482.60	8,048.52	110.05
Objective 2	6,300.94	342.96	6,643.90	111.20
Objective 3	6,456.22	279.32	6,735.54	119.79
Objective 4	6,300.96	286.94	6,587.90	111.22

Based on the results of the optimized lateral path and the optimized vertical profile for four objectives, four 4D optimization trajectories are obtained of commercial flight as shown in Figure 13. In Figure 13, The lateral optimized paths and the vertical optimized profiles are combined to obtain 3D trajectories, which are added the flight time on each waypoint to generate 4D trajectories. They are more intuitive and clear than the results of traditional trajectory optimization.

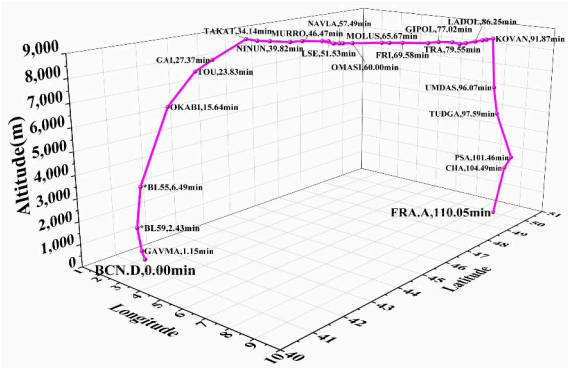

(a) The 4D trajectory of Objective 1

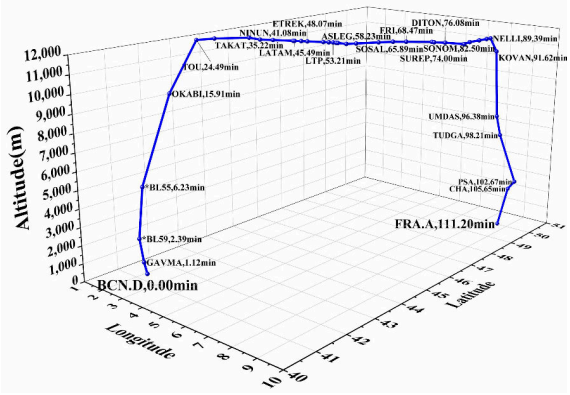

(b) The 4D trajectory of Objective 2

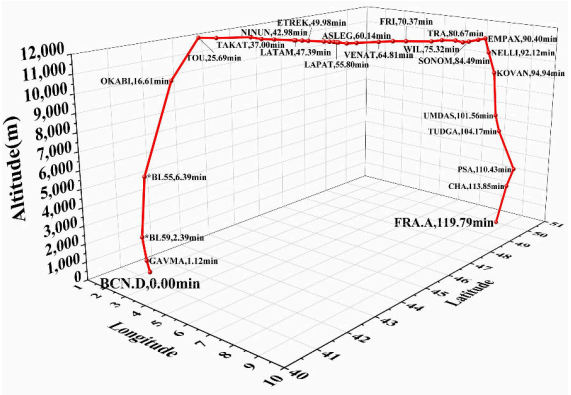

(c) The 4D trajectory of Objective 3

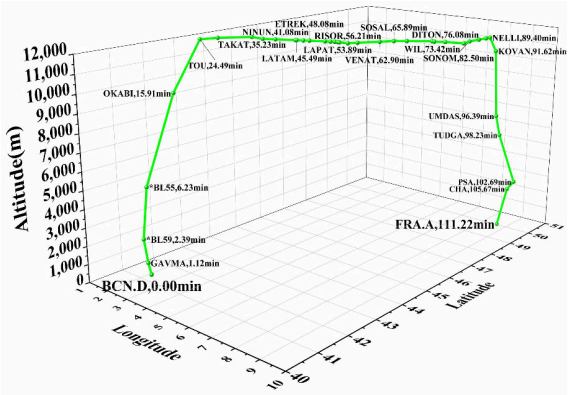

(d) The 4D trajectory of Objective 4

FIGURE 13. **The multi-objective 4D optimization trajectories of commercial flight.**

Through the data such as the longitude and latitude coordinates of sectors' boundary, the height of sector, the longitude and latitude coordinates and heights of 4D optimization trajectories' waypoints and the flight time at each waypoint, the visual simulation of four 4D optimization trajectories is realized as shown in Figure 14.

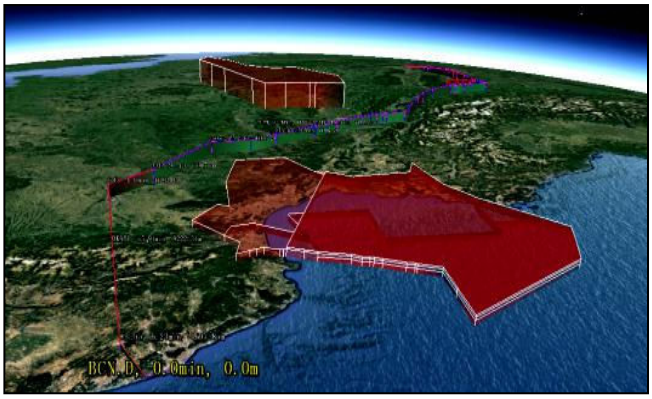

FIGURE 14. **The visual simulation of 4D optimization trajectories on Google Earth.**

C. SENSITIVITY STUDY

This paper conducts a sensitivity study on the objective function for the minimum total cost in the vertical profile optimization to analyze the impact of conventional cost and environmental cost on the optimization of the total cost. Set weight θ as the sensitivity coefficient of conventional cost, then $(1-\theta)$ as the sensitivity coefficient of the environmental cost, $0 \le \theta \le 1$. R represents the reduction rate of conventional cost, environmental cost, and total cost for Objective 4 (the minimum total cost) compared with Objective 1 (the shortest flight time). The results of the sensitivity study are shown in Figure 15.

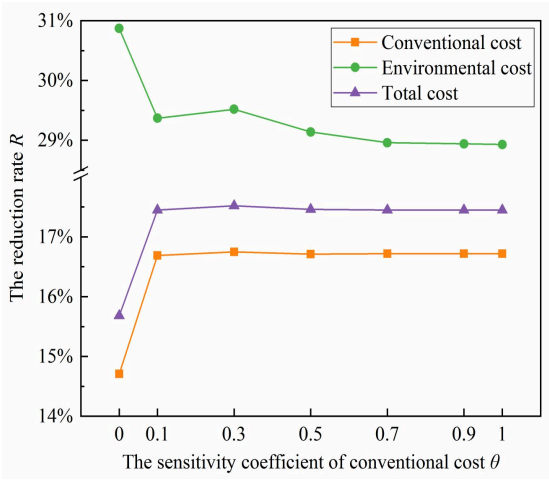

FIGURE 15. **The results of the sensitivity study.**

Figure 15 shows that the overall trend of the reduction rate of total cost increases gradually with the increase of the weight θ of the conventional cost, indicating that conventional cost is still an important objective for trajectory optimization, and the factor of conventional cost cannot be ignored in the process of green trajectory optimization. As shown in Figure 16, in order to establish the green trajectory, it needs to pay the extra conventional cost, but the sensitivity coefficient $(\theta = 0.3)$ can be found to make the balanced costs of conventional cost and environmental cost for the optimal

total cost using the trajectory optimization tool constructed in this paper.

V. CONCLUSION

For green civil aviation, this paper proposes a method for 4D trajectory optimization of commercial flight to compare and analyze the relationship between environmental cost and conventional cost. First of all, the trajectory optimization framework is constructed by the aircraft dynamics, the aircraft performance, the air route structure, the meteorology, and the conventional cost. Some state-of-the-art methods such as LIM, RCM, AM, and intersection method for line segment and rectangle are applied innovatively to process the data of air route structure and weather.

Based on the trajectory optimization framework, the concept of green trajectory is put forward. The objective functions for green civil aviation are proposed combined with the models of greenhouse gas cost and harmful gas cost. In order to optimize the lateral path and vertical profile, the A* algorithm and the trapezoidal collocation method are used respectively.

A case study of the A320 from the Barcelona Airport to Frankfurt Airport on a typical time reveals:

(1) After the optimization, the optimal conventional cost, the optimal environmental cost, and the optimal total cost can be obtained under different objectives. If the optimization of conventional cost is only considered, the optimal environmental cost cannot be got.

(2) According to the sensitivity study, when constructing the green optimization trajectory, the conventional costs such as fuel cost, time cost, and en route charge cannot be ignored, and the total cost can be more optimized by adjusting the weights of environmental cost and conventional cost.

On the account of the optimization results, the visual simulations are displayed in this paper as well. This paper analyzes the impact of multi-objective on 4D trajectory optimization, improving a computer-aided tool for 4D trajectory optimization for green civil aviation, so as to provide guidance and reference for the construction of flight trajectory. Lateral paths and vertical profiles are optimized separately in this paper, and the 3D optimization method integrating two dimensions of lateral and vertical can be tried in future work.

REFERENCES

[1] K. Kleiner, "Civil aviation faces green challenge," *Nature*, vol. 448, no. 7150, pp. 120-121, July 2007.

[2] Y. Glina, S. Troxel, T. Reynolds, and M. McPartland, "Wind information requirements to support four dimensional trajectory-based operations," in *Proc. 12th AIAA Aviation Technol., Integration, and Operations (ATIO) Conf. and 14th AIAA/ISSMO*, Indianapolis, Indiana, USA, Sep. 17-19, 2012, pp. 1-14.

[3] S. Vilardaga and X. Prats, "Operating cost sensitivity to required time of arrival commands to ensure separation in optimal aircraft 4D trajectories," *Transp. Res. Part C Emerg. Technol.*, vol. 61, pp. 75-86, 2015.

[4] X. Prats, V. Puig, and J. Quevedo, "A multi-objective optimization strategy for designing aircraft noise abatement procedures. Case study at Girona airport," *Transp. Res. Part D Transp. Environ.*, vol. 16, no. 1, pp. 31-41, 2011.

[5] L. Chapman, "Transport and climate change: a review," *Journal of Transport Geography*, vol. 15, no. 5, pp. 354-367, September 2007.

[6] W. Yang, "Global governance on international aviation emissions: a multidimensional approach," Ph.D. dissertation, Jilin University, Jilin, China, 2014.

[7] K. Gierens, L. Lim, and K. Eleftheratos, "A Review of various strategies for contrail avoidance," *The Open Atmospheric Science Journal*, vol. 2, no. 1, pp. 1-7, February 2008.

[8] A. J. Timmis, A. Hodzic, L. Koh, M. Bonner, C. Soutis, A. W. Schäfer, and L. Dray, "Environmental impact assessment of aviation emission reduction through the implementation of composite materials," *The International Journal of Life Cycle Assessment*, vol. 20, no. 2, pp. 233-243, 2015.

[9] K. Moolchandani, P. Govindaraju, S. Roy, W. A. Crossley, and D. A. DeLaurentis, "Assessing effects of aircraft and fuel technology advancement on select aviation environmental impacts," *Journal of Aircraft*, vol. 54, no. 3, pp.1-13, 2017.

[10] Z. Wei and C. Wang, "Estimating method of pollution emissions for scheduled flight in different phases," *Journal of Traffic and Transportation Engineering*, vol. 10, no. 6, pp. 48-52, December 2010.

[11] P. Phleps and M. Hornung, "Noise and emission targeted economic trade-off for next generation single-aisle aircraft," *Journal of Air Transport Management*, vol. 26, pp. 14-19, 2013.

[12] M. Soler, B. Zou, and M. Hansen, "Contrail sensitive 4D trajectory planning with flight level allocation using multiphase mixed-integer optimal control," in *Proc. AIAA Guidance, Navigation, and Control (GNC) Conf.*, Boston, MA, USA, Aug. 2013, pp. 1-19.

[13] N. Y. Chen, B. Sridhar, H. K. Ng, and J. H. Li, "Evaluation of contrail reduction strategies based on environmental and operational costs," in *Proc. AIAA Guidance, Navigation, and Control (GNC) Conf.*, Minneapolis, Minnesota, USA, Aug. 2012, pp. 1-9.

[14] N. Y. Chen, B. Sridhar, H. K. Ng, and J. H. Li, "Evaluating tradeoff between environmental impact and operational costs for enroute air traffic," in *Proc. AIAA Guidance, Navigation, and Control (GNC) Conf.*, National Harbor, Maryland, USA, Jan. 2014, pp. 1-10.

[15] D. G. Hull, *Fundamentals of airplane flight mechanics*, Springer, Berlin, Heidelberg, Germany, 2007, pp. 20-23.

[16] R. Chamlou, "Design principles and algorithm development for two types of NextGen airborne conflict detection and collision avoidance," in *Proc. Integrated Communications Navigation & Surveillance Conf.*, Herndon, VA, USA, May 2010, N7-1-N7-12.

[17] Q. Mou and C. Wang, "Assignment model and algorithm for solution of the optimization use of flight level," *Journal of University of Electronic Science and Technology of China*, vol. 38, no. 4, pp. 573-577, July 2009.

[18] Y. Lu, "Research on the initial flight plan 4D trajectory generating and simulation system," Master thesis, Nanjing University of Aeronautics and Astronautics, Nanjing, China, 2014.

[19] S. Wan, Y. Xia, L. Qi, Y. Yang, and M. Atiquzzaman, "Automated colorization of a grayscale image with seed points propagation," *IEEE Transactions on Multimedia*, 2020.

[20] S. Ding, S. Qu, Y. Xi, and S. Wan, "Stimulus-driven and concept-driven analysis for image caption generation," *Neurocomputing*, 2019.

[21] S. Wan, Y. Zhao, T. Wang, Z. Gu, Q. H. Abbasi, and K. K. R. Choo, "Multi-dimensional data indexing and range query processing via Voronoi diagram for internet of things," *Future Generation Computer Systems*, vol. 91, pp. 382-391，February 2019.

[22] Y. Zhao, H. Li, S. Wan, A. Sekuboyina, X. Hu, G. Tetteh, M. Piraud, and B. Menze, "Knowledge-aided convolutional neural network for small organ segmentation," *IEEE Journal of Biomedical and Health Informatics*, vol. 23, no. 4. pp. 1363-1373, July 2019.

[23] Z. Gao, H. Z. Xuan, H. Zhang, S. Wan, and K. K. R. Choo, "Adaptive fusion and category-level dictionary learning model for multiview human action recognition," *IEEE Internet of Things Journal*, vol. 6, no. 6, pp. 9280-9293, December 2019.

[24] S. Wan, Z. Gu, and Q. Ni, "Cognitive computing and wireless communications on the edge for healthcare service robots", *Computer Communications*, vol. 149, pp. 99-106, January 2020.

[25] V. Williams, R. B. Noland, and R. Toumi, "Air transport cruise altitude restrictions to minimize contrail formation," *Climate Policy*, vol. 3, no. 3, pp. 207-219, 2003.
[26] S. E. Campbell, N. A. Neogi, and M. B. Bragg, "An operational strategy for persistent contrail mitigation," in *Proc. 9th AIAA Aviation Technology, Integration, and Operations (ATIO) Conf.* , Hilton Head, South Carolina, USA, September 2009, pp. 1-14.
[27] B. Sridhar, N. Y. Chen, and H. K. Ng, "Fuel efficient strategies for reducing contrail formations in United States airspace," in *Proc. Digital Avionics Systems Conf.*, Salt Lake City, UT, USA, October 2010.
[28] A. J. Torija, R. H. Self, "Aircraft classification for efficient modelling of environmental noise impact of aviation," *Journal of Air Transport Management*, vol. 67, pp. 157-168, 2018.
[29] A. Rodríguez-Díaz, B. Adenso-Díaz, and P. L. González-Torre, "Improving aircraft approach operations taking into account noise and fuel consumption," *Journal of Air Transport Management*, vol. 77, pp. 46-56, 2019.
[30] R. Amin and S. Alam, "A heuristic search approach to find contrail avoidance flight routes," in *Proc. 28th Australasian Joint Conf.*, Canberra, ACT, Australia, November 2015.
[31] A. Alizadeh, M. Uzun, and E. Koyuncu, "Optimal trajectory planning based on wind-optimal cost index," in *Proc. Aviation Technology, Integration, and Operations Conf.*, Atlanta, Georgia, USA, June 2018.
[32] M. Kelly, "An introduction to trajectory optimization: how to do your own direct collocation," *SIAM Review*, vol. 59, no. 4, pp. 849-904, 2017.
[33] R. D. Codina, "Optimal trajectory management for aircraft descent operations subject to time constraints," Ph.D. dissertation, Technical University of Catalonia-BarcelonaTech, Barcelona, Spain, 2019.
[34] S. Hartjes, M. E. G. van Hellenberg Hubar, and H. G. Visser, "Multiple-phase trajectory optimization for formation flight in civil aviation," *CEAS Aeronaut. Journal*, vol. 10, no. 2, pp. 453–462, 2019.
[35] Y. Tian, L. Wan, B. Ye, and D. Xing, "Cruise flight performance optimization for minimizing green direct operating cost, " *Sustainability*, vol. 11, no.14, 2019.
[36] Z. Fang, *Aircraft Flight Dynamics*, Beihang University Press, Beijing, China, 2005, pp. 1-35.
[37] *Mode Accuracy Summary Report for the Base of Aircraft Data(BADA) REVISION 3.11*, EUROCONTROL Experimental Center, EEC: Bretigny, France, 2012, pp. 7-28.
[38] S. Ruiz, L. Guichard, N. Pilon, and K. Delcourte, "A new air traffic flow management user-driven prioritisation process for low volume operator in constraint: simulations and results," *Journal of Advanced Transportation*, vol. 2019, 2019.
[39] *Customer Guide to Charges*, Central Route Charge Office EUROCONTROL, Belgium, 2019, pp. 31.
[40] *Aviation Environmental Design Tool(AEDT) Technical manual Version 2c*, Department of Transportation Federal Aviation Administration, USA, 2016, pp. 188-191.
[41] N. Y. Chen, B. Sridhar, and H. K. Ng, "Tradeoff between Contrail Reduction and Emissions in United States National Airspace," *Journal of Aircraft*, vol. 49, no. 5, pp. 1367-1375, 2012.
[42] *Annex 16 "International standards and recommended practices, Environmental protection", Volume II "Aircraft engine emissions", 3rd edition*, ICAO, Canada, 2008.
[43] Y. Tian, L. Wan, K. Han, and B. Ye, "Optimization of terminal airspace operation with environmental considerations," *Transp. Res. Part D Transp. Environ.*, vol. 63, pp. 872-889, 2018.
[44] M. Greenstone, E. Kopits, and A. Wolverton, "Developing a social cost of carbon for US regulatory analysis: a methodology and interpretation," *Review of Environmental Economics and Policy*, vol. 7, no. 1, pp. 23-46, 2013.

YONG TIAN was born in Honghu, China, in 1976. He received the Ph.D. degree in transportation planning and management from the Nanjing University of Aeronautics and Astronautics, in 2009, where he started working as an Associate Professor, in 2000. His research interests include air traffic management and airspace planning.

XIUQI HE was born in Chengdu, China, in 1994. He is currently pursuing the master degree in safety science and engineering with the Nanjing University of Aeronautics and Astronautics. He joined Mianyang Branch of Civil Aviation Flight University of China, in 2017. His research interests include green civil aviation technology and aircraft trajectory optimization.

YAN XU was born in Nanjing, China, in 1990. He is a Lecturer at Cranfiled Univiersity, with the School of Aerospace, Transport and Manufacturing. He conducted postdoctoral research in the same school in 2018-2019. Prior to joining Cranfield, he received his Ph.D. in Aerospace Science and Technology from the Technical University of Catalonia in 2018, and M.Sc. and B.Eng. in Traffic Engineering from Nanjing University of Aeronautics and Astronautics in 2015 and 2012. His main research interests include air traffic flow management, aircraft trajectory optimization and UAV traffic management.

LILI WAN was born in Dongtai, China, in 1981. She received the Ph.D. degree in transportation planning and management from the Nanjing University of Aeronautics and Astronautics, in 2016, where she started working as a Lecturer, in 2005. Her research interests include air traffic management and airspace planning.

BOJIA YE was born in Nanjing, China, in 1983. He received the Ph.D. degree in transportation planning and management from the Nanjing University of Aeronautics and Astronautics, in 2013, where he started working as a Lecturer, in 2013. His research interests include air traffic management and artificial intelligence.

4D trajectory optimization of commercial flight for green civil aviation

Tian, Yong

2020-03-31

Tian Y, He X, Xu Y, et al., (2020) 4D trajectory optimization of commercial flight for green civil aviation. IEEE Access, Volume 8, 2020, pp. 62815-62829
https://doi.org/10.1109/ACCESS.2020.2984488